

4-2-2009

Aqueous Phase C-H Bond Oxidation Reaction of Arylalkanes Catalyzed by a Water-Soluble Cationic Ru(III) Complex $[(\text{pymox-Me}_2)_2\text{RuCl}_2]^+\text{BF}_4^-$

Chae S. Yi

Marquette University, chae.yi@marquette.edu

Ki Hyeok Kwon

Marquette University

Do W. Lee

Marquette University

Aqueous Phase C-H Bond Oxidation Reaction of Arylalkanes Catalyzed by a Water-Soluble Cationic Ru(III) Complex $[(\text{pymox-Me}_2)_2\text{RuCl}_2]^+\text{BF}_4^-$

Chae S. Yi

*Department of Chemistry, Marquette University,
Milwaukee, WI*

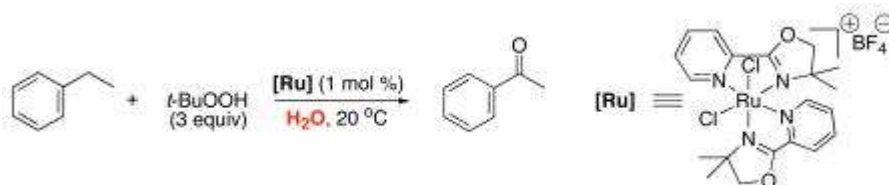
Ki-Hyeok Kwon

*Department of Chemistry, Marquette University,
Milwaukee, WI*

Do W. Lee

*Department of Chemistry, Marquette University,
Milwaukee, WI*

Abstract

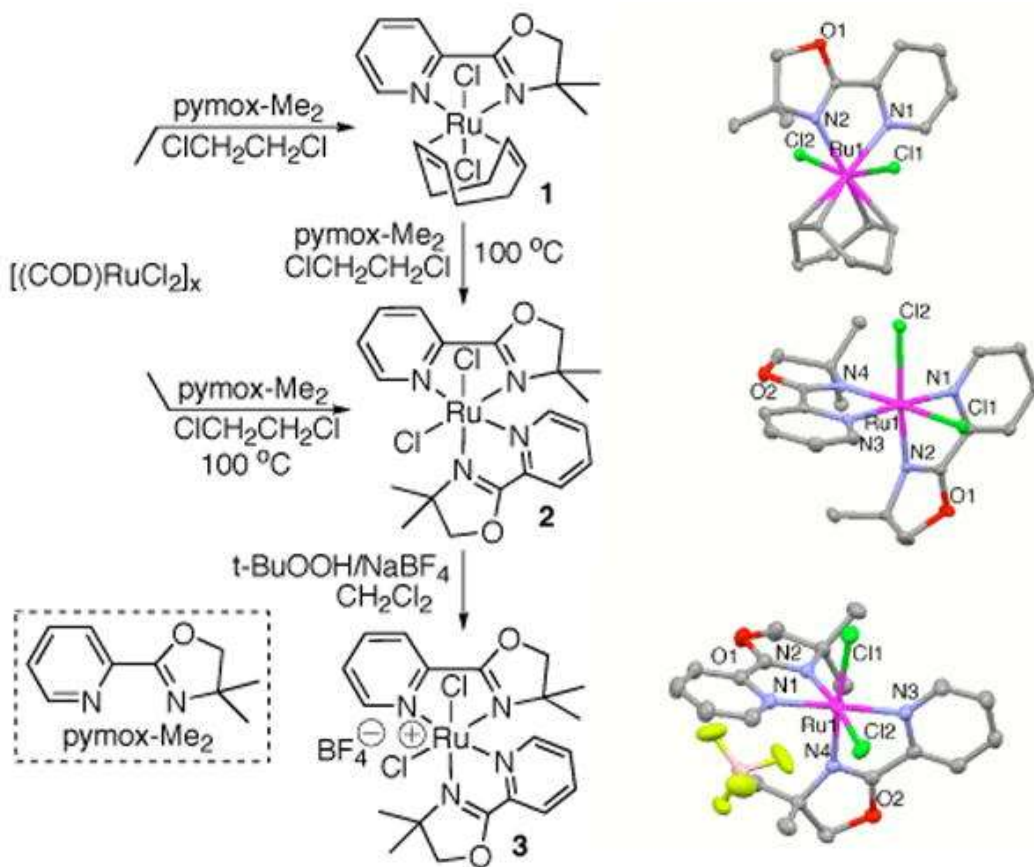


The cationic complex [(pymox-Me₂)RuCl₂]⁺BF₄⁻ was found to be a highly effective catalyst for the C-H bond oxidation reaction of arylalkanes in water. For example, the treatment of ethylbenzene (1.0 mmol) with *t*-BuOOH (3.0 mmol) and 1.0 mol % of the Ru catalyst in water (3 mL) cleanly produced PhCOCH₃ at room temperature. Both a large kinetic isotope effect ($k_H/k_D = 14$) and a relatively large Hammett value ($\rho = -1.1$) suggest a solvent-caged oxygen rebounding mechanism via a Ru(IV)-oxo intermediate species.

Aqueous phase homogeneous catalysis has emerged as an important tool for attaining new "green" chemical technology in both industrial and fine chemical processes.¹ Particular attention has been centered on the development of water-soluble metal catalysts for the C-H bond oxidation reactions, and in this regard, late transition metal complexes with nitrogen ligands have been shown to be effective for mediating catalytic oxidation of saturated hydrocarbons in protic media.² A number of chemoselective allylic and propargylic C-H bond oxidation and oxidative coupling reactions of amines have recently been achieved by using water-soluble dirhodium³ and ruthenium⁴ catalysts, respectively. Fukuzumi reported an efficient C-H bond oxidation of arylalkanes mediated by CAN/[Ru(tpa)(H₂O)₂]⁺ system in aqueous media.⁵ Li and co-workers devised a number of oxidative coupling reactions involving C-H bond activation in water.⁶ Surface-modified heterogeneous ruthenium-hydroxo catalysts have also been found to mediate selective oxidation of benzylamines to arylamides in water.⁷ Despite these recent advances, only a few well-defined synthetic metal catalysts have been shown to mediate aerobic C-H bond oxidation reactions in the aqueous phase, and considerable controversies still persist on the issues of reaction mechanisms and the nature of reactive species.

As part of an on-going effort to develop ruthenium-catalyzed C-H bond activation reactions,⁸ we initially screened several chelating nitrogen ligands to synthesize water-soluble ruthenium catalysts. Thus, the treatment of [(COD)RuCl₂]_x with 1.2 equivalents of 4,4-

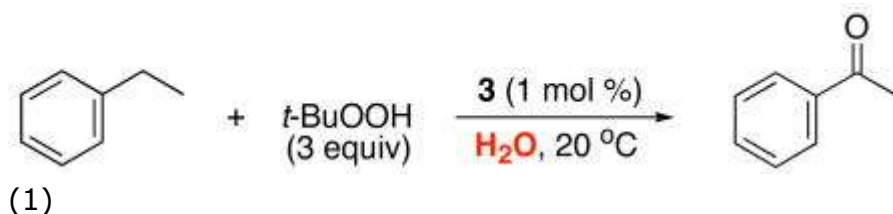
dimethyl-2-(2-pyridyl)oxazoline (pymox-Me₂) ligand in 1,2-dichloroethane at 50 °C produced an orange-yellow colored complex (pymox-Me₂)Ru(COD)Cl₂ (**1**), which was isolated in 65% yield after recrystallization in *n*-hexanes/CH₂Cl₂ (Scheme 1). The treatment of **1** (0.4 mmol) with pymox-Me₂ (1.9 mmol) in 1,2-dichloroethane at 100 °C led to the isolation of a deep blue-purple colored complex (pymox-Me₂)₂RuCl₂ (**2**) in 55% yield. Alternatively, the complex **2** could be directly produced from the treatment of [(COD)RuCl₂]_x with excess amount of pymox-Me₂ in 1,2-dichloroethane at 100 °C (65% yield).



Scheme 1

The subsequent treatment of **2** with NaBF₄ and *t*-BuOOH in CH₂Cl₂ led to the cationic Ru(III) complex [(pymox-Me₂)₂RuCl₂]⁺BF₄⁻ (**3**) in 73% isolated yield. The structure of these ruthenium complexes was completely established by both spectroscopic and X-ray crystallographic methods. The molecular structure of both **2** and **3**

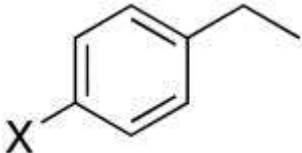
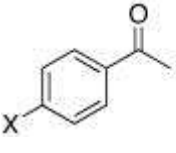
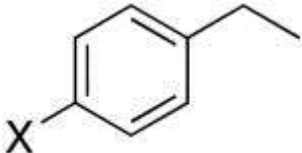
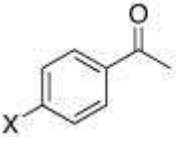
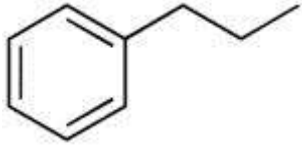
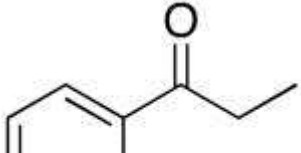
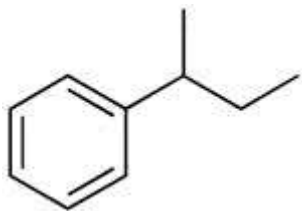
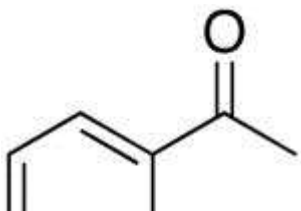
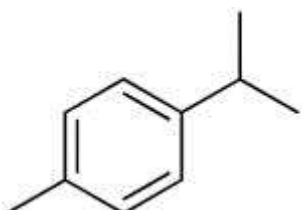
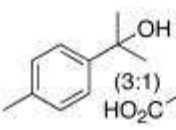
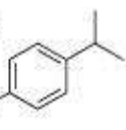
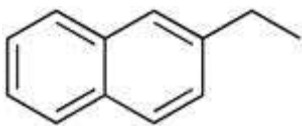
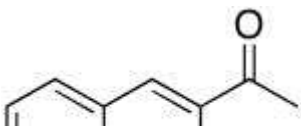
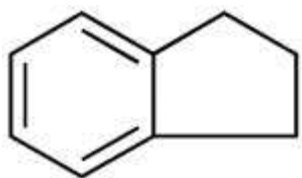
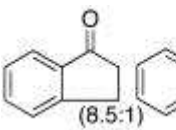
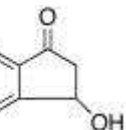
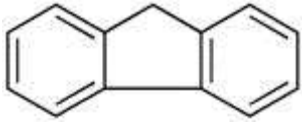
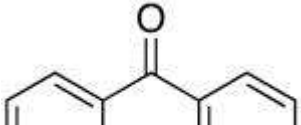
showed an octahedral geometry with cis coordination of the chloride and anti pyridine ligands. The average Ru-Cl bond distance of the cationic Ru(III) complex **3** (2.33 Å) was found to be considerably shorter than the neutral complex **2** (2.41 Å). The magnetic moment of **3** ($\mu_{\text{eff}} = 1.55 B_M$) as determined by using the Evans NMR method was also consistent with a paramagnetic Ru(III) complex.⁹

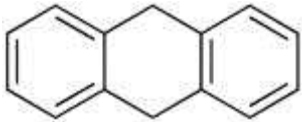
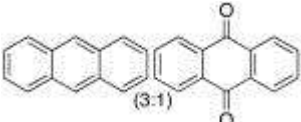
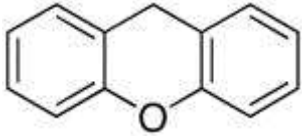
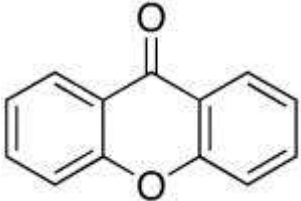
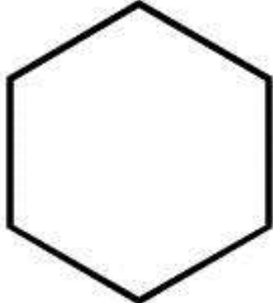
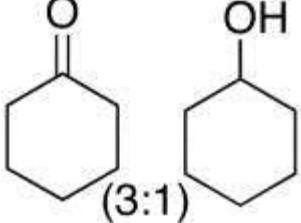
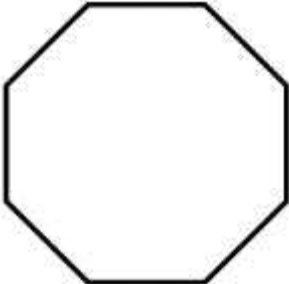
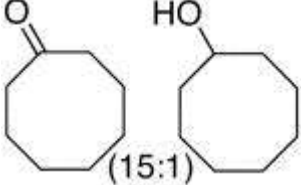


In a strikingly different reactivity pattern, only the complex **3** was found to exhibit high catalytic activity for the C-H bond oxidation reaction in aqueous solution, even though both **2** and **3** are soluble in water. Thus, the treatment of ethylbenzene (1.0 mmol) with *t*-BuOOH (3 mmol, 70 wt % in aqueous solution) in the presence of 1 mol % of **3** in water (3 mL) cleanly produced PhCOCH₃ in >95% conversion within 16 h at room temperature (eq 1). Salient features of the catalyst **3** are that it retains significant activity after repeated runs (61% yield after third run), and it can be readily separated from the reaction mixture by simple extraction.

The scope of the oxidation reaction was surveyed by using **3** as the catalyst (Table 1). In general, the C-H bond oxidation of benzylic compounds occurred smoothly at room temperature to give the ketone products. The formation of C-C bond cleavage product for isobutylbenzene is reminiscent of the oxidation reaction promoted by transition metal complexes (entry 5), where benzyloxy radical species has been implicated for the C-C bond cleavage reactions of alkylbenzenes.¹⁰ The oxidation of tertiary benzylic C-H bond is favored over the primary ones to give the alcohol product (entry 6). The dehydrogenation product was favored over the oxidation product for the 9,10-anthracene case (entry 10). The oxidation of cyclic alkanes was found to be sluggish, giving only modest conversions under the similar reaction conditions (entry 12, 13).

Table 1. Aqueous Phase C-H Bond Oxidation of Arylalkanes.^a

entry	substrate	product(s)	t (h)	convn (%)	yield (%) ^b
1			16	95	83(90)
2		 X = H X = OMe X = Cl	16	97	87(95)
3			16	87	77(83)
4					16
5			24	56	41(47)
6		 (3:1)  HO ₂ C	16	90	74(80) ^c
7			16	94	89(90)
8		 (8.5:1)  OH	2	>99	80(90) ^d
9 ^e			2	93	86(92)

entry	substrate	product(s)	t (h)	convn (%)	yield (%) ^b
10 ^e			2	>99	88(95)
11 ^e			2	>99	87(95)
12			24	33	--(29) ^f
13			24	66	54(62)

^aReaction conditions: substrate (1.0 mmol), *t*-BuOOH (3.0 mmol, 70 wt % in water), **3** (1.0 mol %), H₂O (3 mL), 20-22 °C.

^bIsolated product yields. The GC product yields are listed in parenthesis.

^c<5% of bezaldehyde derivative is formed.

^d5% of 1,3-indandione is formed.

^eThe substrate was dissolved in 1 mL of CH₂Cl₂.

^fThe products were not isolated due to low conversion and difficulty in separation.

We performed the following experiments to gain further mechanistic insights on the oxidation reaction. (1) A very large kinetic isotope effect of $k_H/k_D = 14$ was obtained from the pseudo-first order plots of the oxidation reaction of ethylbenzene vs ethylbenzene-*d*₁₀ at 20 °C ($k_{\text{obs}} = 2.1 \times 10^{-2} \text{ h}^{-1}$ and $1.5 \times 10^{-3} \text{ h}^{-1}$, respectively) ([Figure S1, Supporting Information](#)).⁹ Such a large deuterium isotope effect has been rarely observed in C-H bond oxidation reactions mediated by synthetic metal catalysts, but more commonly observed in enzyme-

catalyzed oxidation reactions where quantum mechanical tunneling effect has been ascribed to effect the rate-limiting C-H activation step.¹¹

(2) The Hammett correlation of *para*-substituted ethylbenzene substrates $p\text{-X-C}_6\text{H}_4\text{CH}_2\text{CH}_3$ (X = OMe, CH₃, H, F, Cl) led to $\rho = -1.1$ (Figure 1). The observed ρ value is substantially higher than the oxidation reactions catalyzed by free radical species such as *t*-BuO• and *t*-BuOO• ($\rho = -0.4$ to -0.6), but somewhat lower than the ones catalyzed by (PPh₃)₃RuCl₂/*t*-BuOOH and cytochrome P-450 and their synthetic model systems ($\rho = -1.3$ to -1.6).¹² A relatively high $-\rho$ value suggested of a substantial charge transfer from a metal-oxo species to the substrate during the C-H bond cleavage step.

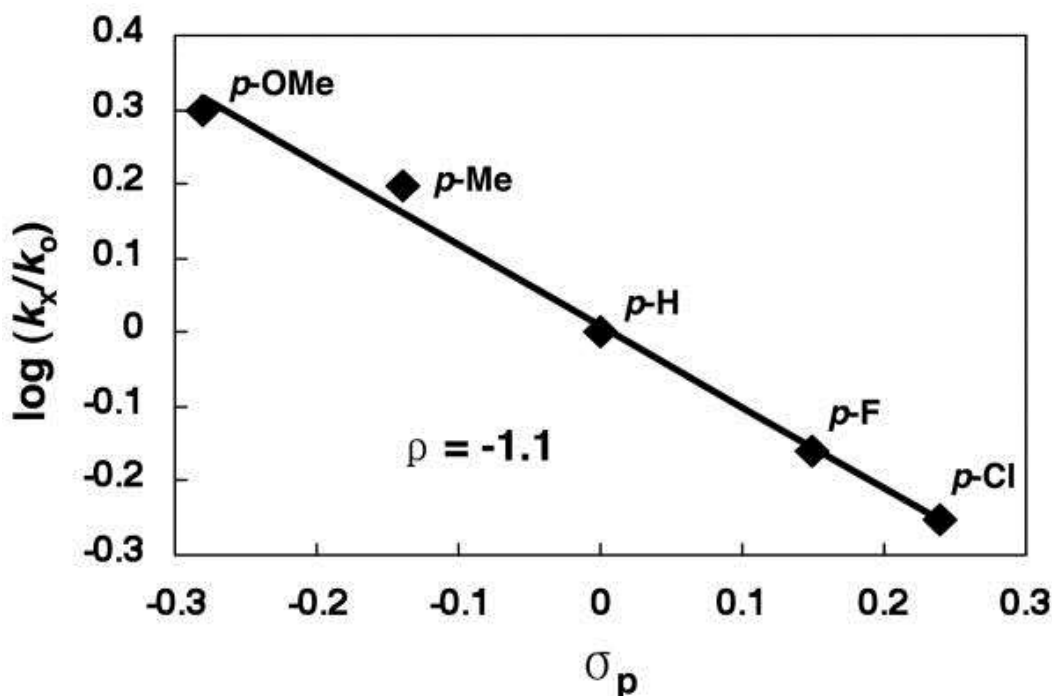


Figure 1. Hammett plot for the oxidation reaction of $p\text{-X-C}_6\text{H}_4\text{CH}_2\text{CH}_3$ (X = OMe, CH₃, H, F, Cl) in water.

(3) The initially inactive **2** became an active catalyst upon addition of NaBF₄ for the oxidation reaction. This fact and a relatively low Ru(II)/Ru(III) redox potential ($E_0 = +0.22$ V) clearly indicate that the cationic Ru(III) complex is the catalytically active species for the oxidation reaction.¹³ The observation of a strong metal-to-ligand charge transfer band at 360 nm ($d\pi\text{-}\pi^*$) from the reaction mixture of

2 with *t*-BuOOH and NaBF₄ also supports the formation of a Ru(III) species ([Figure S2, Supporting Information](#)). These data are most consistent with a "solvent-caged" oxygen rebound mechanism of the rate-limiting C-H oxidation step from a Ru(IV)-oxo species.^{12,13} The fact that a radical scavenger TEMPO (10 mol %) did not significantly affected the rate of the oxidation reaction also supports the notion of a solvent-caged mechanism.

In summary, the cationic Ru(III) complex **3** was found to be a highly effective catalyst for the benzylic C-H bond oxidation reaction in water. While high valent metal-oxo species have been invoked in both non-heme and Gif-type oxidations,^{2b,14} catalytic C-H bond oxidation reactions mediated by well-defined Ru(III) complexes have been rarely reported.¹³ Efforts are currently underway to extend the scope of the oxidation reaction as well as to establish the nature of reactive species.

Acknowledgments

Financial support from the National Institute of Health, General Medical Sciences (R15 GM55987) is gratefully acknowledged). We also thank Dr. Sergey Lindeman (Marquette University) for X-ray crystallographic determination of the ruthenium complexes.

Footnotes

[Supporting Information](#) Available: Experimental procedures and crystallographic data of **1**, **2** and **3** (23 pages, print/PDF). This material is available free of charge via the Internet at <http://pubs.acs.org>.

References

- ¹Recent reviews and monographs: **(a)** Lindström UM. Chem Rev. 2002;102:2751–2772. **(b)** Cornils B, Hermann WA, editors. Aqueous-Phase Organometallic Catalysis. Wiley-VCH; Weinheim: 2004. **(c)** Cornils B, Hermann WA, Horváth IT, Leitner W, Mecking S, Olivier-Bourbigou H, Vogt D, editors. Multiphase Homogeneous Catalysis. Vol. 1 Wiley-VCH; Weinheim: 2005. **(d)** Li CJ. Chem Rev. 2005;105:3095–3166.
- ²**(a)** Sen A, Lin M. Chem Commun. 1992:509–510. **(b)** Barton DHR, Doller D. Acc Chem Res. 1992;25:504–512. **(c)** Periana RA, Taube DJ, Gamble S, Taube H, Satoh T, Fujii H. Science. 1998;280:560–564.

- ³**(a)** Doyle MP, Choi H. *Org Lett.* 2007;9:5349–5352. **(b)** McLaughlin EC, Doyle MP. *J Org Chem.* 2008;73:4317–4319.
- ⁴Murahashi SI, Zhang D. *Chem Soc Rev.* 2008;37:1490–1501.
- ⁵Hirai Y, Kojima T, Mizutani Y, Shiota Y, Yoshizawa K, Fukuzumi S. *Angew Chem, Int Ed.* 2008;47:5772–5776.
- ⁶**(a)** Li CJ. *Acc Chem Res.* 2002;35:533–538. **(b)** Herrerías CI, Yao X, Li Z, Li CJ. *Chem Rev.* 2007;107:2546–2562.
- ⁷Kim JW, Yamaguchi K, Mizuno N. *Angew Chem, Int Ed.* 2008;47:9249–9251.
- ⁸**(a)** Yi CS, Yun SY. *J Am Chem Soc.* 2005;127:17000–17006. **(b)** Yi CS, Zhang J. *Chem Commun.* 2008:2349–2351.
- ⁹See the [Supporting Information](#) for experimental details.
- ¹⁰**(a)** Sheldon RA, Kochi JK. *Metal-Catalyzed Oxidations of Organic Compounds.* New York: Academic Press; 1981. **(b)** Sawyer DT, Sobkowiak A, Matsushita T. *Acc Chem Res.* 1996;29:409–416.
- ¹¹**(a)** Glickman MH, Wiseman JS, Klinman JP. *J Am Chem Soc.* 1994;116:793–794. **(b)** Jonsson T, Glickman MH, Sun S, Klinman JP. *J Am Chem Soc.* 1996;118:10319–10320. **(c)** Ambundo EA, Friesner RA, Lippard SJ. *J Am Chem Soc.* 2002;124:8770–8771. **(d)** Pan Z, Horner JH, Newcomb M. *J Am Chem Soc.* 2008;130:7776. **(e)** Gupta A, Mukherjee A, Matsui K, Roth JP. *J Am Chem Soc.* 2008;130:11274–11275.
- ¹²**(a)** Murahashi SI, Komiya N, Oda Y, Kuwabara T, Naota K. *J Org Chem.* 2000;65:9186–9193. **(b)** Che CM, Cheng KW, Chan MCW, Lau TC, Mak CK. *J Org Chem.* 2000;65:7996–8000.
- ¹³For examples of Ru(III)-porphyrin complexes in alkane oxidation reactions, see: Ohtake H, Higuchi T, Hirobe M. *J Am Chem Soc.* 1992;114:10660–10662. **(b)** Groves JT, Bonchio M, Carofiglio T, Shalyaev K. *J Am Chem Soc.* 1996;118:8961–8962.
- ¹⁴**(a)** Que L., Jr *Acc Chem Res.* 2007;40:493–500. **(b)** Nam W. *Acc Chem Res.* 2007;40:522–531.

Supplementary Material

Supporting Information

Aqueous Phase C-H Bond Oxidation Reaction of Arylalkanes Catalyzed by a Water-Soluble Cationic Ru(III) Complex [(pymox-Me₂)₂RuCl₂]⁺BF₄⁻

Chae S. Yi*, Ki-Hyeok Kwon and Do W. Lee

Department of Chemistry, Marquette University, Milwaukee, Wisconsin 53201-1881

General Information	S2
Synthesis of 1 , 2 and 3	S2
General Procedure of the Catalytic Reaction	S4
Isotope Effect Study	S5
Hammett Study	S6
Uv-vis Spectra	S7
Cyclic voltammogram of 3	S8
Crystallographic data of 1 , 2 and 3	S9
Selected ¹ H and ¹³ C NMR Spectra	S11

General Information. All operations were carried out in an inert-atmosphere glove box or by using standard high vacuum and Schlenk techniques unless otherwise noted. Tetrahydrofuran, benzene, hexanes and Et₂O were distilled from purple solutions of sodium and benzophenone immediately prior to use. The NMR solvents were dried from activated molecular sieves (4 Å). All organic substrates were received from commercial sources and used without further purification. The ¹H and ¹³C NMR spectra were recorded on a Varian 400 MHz FT-NMR spectrometer. UV-vis spectra were recorded on a Shimadzu UV-1600/1700 instrument. Electrochemical measurements were collected with a BAS CV-50V instrument. The product yields were measured from a Hewlett-Packard HP 6890 GC spectrometer. The elemental analyses were performed at the Midwest MicroLab, Indianapolis, IN.

Synthesis of (pymox-Me₂)Ru(COD)Cl₂ (1). In a glove box, 4,4-dimethyl-2-(2-pyridyl)oxazoline (0.21 g, 1.2 mmol) and [Ru(COD)Cl₂]_x (0.16 g, 0.5 mmol) were dissolved in ClCH₂CH₂Cl (15 mL) in a 25 mL Schlenk tube equipped with a magnetic stirring bar and Teflon stopcock. The reaction tube was brought out of the box, and was stirred in an oil bath at 50 °C for 24 h. After the reaction tube was cooled to room temperature, the volatiles were removed under vacuum, and the residue was recrystallized in CH₂Cl₂/*n*-hexanes to obtain a crude product mixture. The mixture was further purified by flash column chromatography (*n*-hexanes/EtOAc = 4:1) to afford analytically pure product **1** (0.15 g, 65% yield). Single crystals of **1** suitable for X-ray crystallographic analysis were obtained from slow evaporation of CH₂Cl₂ solution.

For **1**: ¹H NMR (400 MHz, CDCl₃) δ 8.05 (ddd, *J* = 5.3, 1.0, 0.7 Hz, py-6-H), 7.86-7.96 (m, 2H, py-3 and 4-H), 7.50 (ddd, *J* = 12.6, 5.3, 2.0 Hz, py-5-H), 5.03 (t, *J* = 2.5 Hz, =CH), 4.52 (t, *J* = 2.6 Hz, =CH), 4.46 (s, 2H, OCH₂), 2.61-2.78 (m, 4H, CH₂), 2.03-2.21 (m, 4H, CH₂), 1.52 (s, 6H, CH₃); ¹³C NMR (100 MHz, CDCl₃) δ 166.6 (N=CO), 150.0, 148.0, 138.2, 128.0 and 126.2 (py), 89.5 and 89.2 (=CH), 82.5 (OCH₂), 70.3 (CCH₃), 30.5 and 29.0 (CH₂), 27.5 (CCH₃); Anal. Calcd for C₁₈H₂₄Cl₂N₂ORu: C, 47.37; H, 5.30. Found: C, 47.13; H, 5.22.

Synthesis of (pymox-Me₂)₂RuCl₂ (2). In a glove box, [Ru(COD)Cl₂]_x (0.20 g, 0.44 mmol) and 4,4-dimethyl-2-(2-pyridyl)oxazoline (0.34 g, 1.94 mmol) were dissolved in ClCH₂CH₂Cl (15 mL) in a 25 mL Schlenk tube equipped with a Teflon stopcock and a magnetic stirring bar. The reaction mixture was stirred in an oil bath at 100 °C for 24 h. After cooling to room temperature, the solvent was removed under vacuum. The residue was recrystallized in CH₂Cl₂/*n*-hexanes to obtain a crude product mixture. The product mixture was further purified by flash chromatography (*n*-hexanes/EtOAc = 4:1) to afford analytically pure product **2** (0.30 g, 65% yield). Alternatively, complex **1** (0.20 g, 0.44 mmol) and pymox-Me₂ (0.34 g, 1.94 mmol) were dissolved in ClCH₂CH₂Cl (15 mL) in a 25 mL Schlenk tube. The reaction mixture was stirred in an oil bath at 100 °C for 24 h. After cooling to room temperature, the solvent was removed under vacuum. The residue was purified by flash column chromatography (*n*-hexanes/EtOAc = 4:1) to afford pure product **2** (0.25 g, 55% yield). Single crystals of **2** suitable for X-ray crystallographic analysis were obtained from CH₂Cl₂/*n*-hexanes solution.

For **2**: ¹H NMR (400 MHz, CDCl₃) δ 10.01 and 10.12 (s, py-6-H), 7.83-7.88 and 7.90-7.95 (m, 2H, py-3 and 4-H), 7.53-7.63 and 7.25-7.39 (m, py-5-H), 4.62 and 4.53 (s, OCH₂), 1.15 and 0.65 (s, CCH₃); ¹³C NMR (100 MHz, CDCl₃) δ 166.8 and 166.5 (N=CO), 156.2, 155.2, 151.6, 151.01, 133.1, 132.9, 132.8, 132.6, 126.1 and 124.9 (py), 83.4 and 82.7 (OCH₂), 70.6 and 70.3 (CCH₃), 28.2 and 27.1 (CCH₃); Anal. Calcd for C₂₀H₂₄Cl₂N₄O₂Ru: C, 45.81; H, 4.61. Found C, 44.92; H, 4.54.

Synthesis of [(pymox-Me₂)₂RuCl₂]⁺BF₄⁻ (3). In a 25 mL Schlenk tube equipped with a Teflon stopcock and a magnetic stirring bar, the complex **2** (100 mg, 0.19 mmol), NaBF₄ (90 mg, 0.95 mmol) and *t*-BuOOH (5.5 M in decane, 0.42 mL, 1.9 mmol) were dissolved in CH₂Cl₂ (5 mL). The reaction mixture was stirred for 5 h at room temperature. The solvent was removed under vacuum. The residue was recrystallized in CH₂Cl₂/*n*-hexanes to obtain the product **3** (85 mg, 73% yield). Single crystals of complex **3** suitable for X-ray crystallographic analysis were obtained from CH₂Cl₂/*n*-hexanes solution. The Evans NMR method was used to measure the

magnetic moment of the complex by following the experimental procedure described in: Girolami, G. S.; Rauchfuss, T. B.; Angelici, R. J. *Synthesis and Technique in Inorganic Chemistry: A Laboratory Manual*, University Science Books: Sausalito, CA, 1999, pp. 125-126.

For **3**: Anal. Calcd for C₂₀H₂₄BCl₂F₄N₄O₂Ru: C, 39.30; H, 3.96. Found C, 38.70; H, 3.77. $\mu_{\text{eff}} = 1.55 B_M$ at 293 K.

General Procedure of the Catalytic Reaction. In air, the complex **3** (6 mg, 10 μmol), an alkane substrate (1.0 mmol) and *t*-BuOOH (70 wt% in H₂O, 0.43 mL, 3.0 mmol) were dissolved in water (3 mL) in a 25 mL Schlenk tube equipped with a magnetic stirring bar. The reaction mixture was stirred at 20 °C for 2-24 h. The reaction tube was opened to air and the solution was extracted with CH₂Cl₂ (10 mL). The solution was filtered through a small pad of silica gel. An internal standard (C₆Me₆, 20 mg) was added to the solution, and the product yield was determined by GC. The ketone product was readily isolated by a column chromatography on silica gel (hexane/EtOAc).

Catalytic Oxidation Reaction of Ethylbenzene with TEMPO. In air, complex **3** (6 mg, 10 μmol) was charged with ethylbenzene (0.12 mL, 1.0 mmol), *t*-BuOOH (70 wt% in H₂O, 0.43 mL, 3.0 mmol), TEMPO (16 mg, 0.1 mmol), H₂O (1.5 mL) and *n*-hexanes (1.0 mL) in a thick-walled 25 mL Schlenk tube equipped with a magnetic stirring bar. The reaction mixture was stirred for 24 h at 20 °C. After the reaction was completed, the reaction tube was opened to air. The solution was extracted with CH₂Cl₂ (10 mL) and organic solution was filtered through a small pad of silica gel. The product yield as determined by GC was 34% (without TEMPO, 40% conversion). It should be noted that *n*-hexanes was added to dissolve TEMPO, and under these biphasic conditions, the reaction rate was considerably lower than in pure water.

Catalyst Recycling Experiment. The complex **3** (6 mg, 10 μmol) was charged with ethylbenzene (0.12 mL, 1.0 mmol), *t*-BuOOH (70 wt% in H₂O, 0.43 mL, 3.0 mmol) and H₂O

(2.5 mL) in a thick-walled 25 mL Schlenk tube equipped with a magnetic stirring bar. The reaction mixture was stirred for 16 h at 20 °C. After the reaction was completed, the reaction tube was opened to air and the solution was extracted with CH₂Cl₂ (10 mL). The extracted solution was filtered through a small pad of silica gel and analyzed by GC. The second and third runs were repeated by using the same aqueous solution. The product yield as determined by GC: 1st run (90%), 2nd run (71%), 3rd run (61%).

Isotope Effect Study. In two separate tubes, complex **3** (6 mg, 10 μmol) was charged with ethylbenzene and ethylbenzene-*d*₁₀ (0.12 mL, 1.0 mmol), *t*-BuOOH (70 wt% in H₂O, 0.43 mL, 3.0 mmol), H₂O (1.5 mL) and *n*-hexanes (1.0 mL) in a 25 mL Schlenk tube equipped with a magnetic stirring bar in air. The reaction tube was stirred at 20 °C. A small portion of the aliquot was drawn periodically from the organic layer, and the product conversion was determined by GC. The *k*_{obs} was obtained from a first-order plot of $-\ln([\text{ethylbenzene}]_t/[\text{ethylbenzene}]_0)$ vs time.

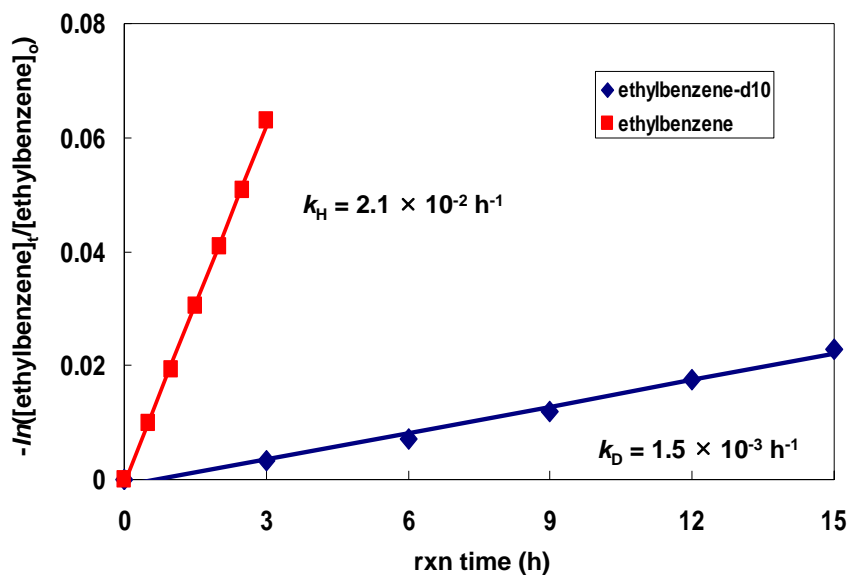


Figure S1. Pseudo first-order plots of $-\ln([\text{ethylbenzene}]_t/[\text{ethylbenzene}]_0)$ vs time.

Hammett Study. In five separate tubes, an equal amount of the complex **3** (6 mg, 10 μmol), $p\text{-X-C}_6\text{H}_4\text{CH}_2\text{CH}_3$ (X = OMe, Me, H, F, Cl) (0.12 mL, 1.0 mmol) and $t\text{-BuOOH}$ (70 wt% in H_2O , 0.43 mL, 3.0 mmol) were dissolved in H_2O (1.5 mL) and $n\text{-hexanes}$ (1.0 mL) in a 25 mL Schlenk tube equipped with a magnetic stirring bar in air. The reaction tubes were stirred at 20 $^\circ\text{C}$. A small portion of the aliquot was drawn periodically from the organic layer, and the conversion was determined by GC. The k_{obs} was estimated from a first-order plot of $-\ln([\text{ArCH}_2\text{CH}_3]_t/[\text{ArCH}_2\text{CH}_3]_0)$ vs time.

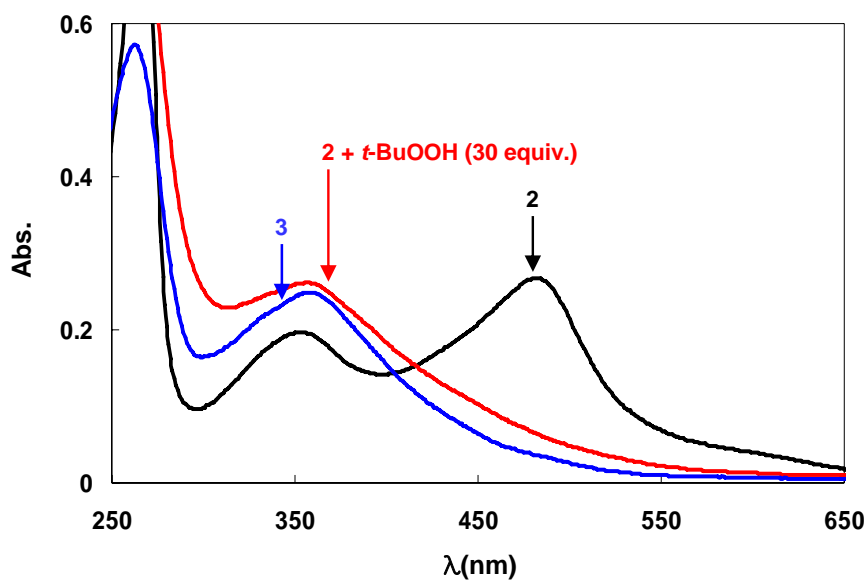


Figure S2. UV-vis spectra of **2** (20 μM), **2** (20 μM) and $t\text{-BuOOH}$ (30 equiv), and **3** (20 μM) in water.

Cyclic Voltammetry of 3. In a volumetric flask, the sample solution was prepared by dissolving complex **3** (10 mg, 1.6 mM) and an electrolyte (0.25 M of Bu₄NPF₆) in 10 mL of CH₂Cl₂. Electrochemical measurements were collected at a scan rate of 200 mV/s from a three-electrode cell composed of a Ag/AgCl electrolyte, a platinum working electrode, and a glassy carbon counter electrode.

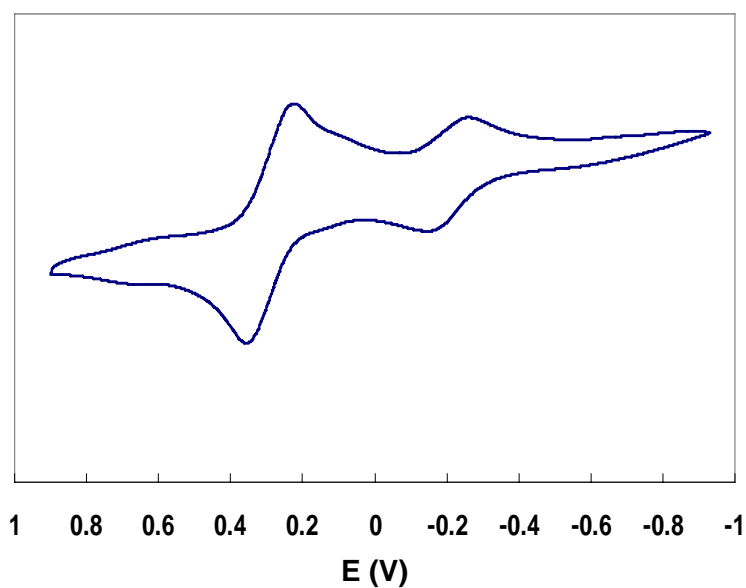


Figure S3. Cyclic voltammogram of **3** in CH₂Cl₂.

Table S1. Crystal data and structure refinement for **1**.

Empirical formula	C _{18.5} H ₂₅ C ₁₃ N ₂ ORu	
Formula weight	498.83	
Temperature	100(2) K	
Wavelength	1.54178 Å	
Crystal system	Monoclinic	
Space group	P2 ₁ /c	
Unit cell dimensions	a = 16.4410(4) Å	α = 90°
	b = 9.8816(3) Å	β = 110.3760(10)°
	c = 12.8838(3) Å	γ = 90°
Volume	1962.17(9) Å ³	
Z	4	
Density (calculated)	1.689 Mg/m ³	
Absorption coefficient	10.305 mm ⁻¹	
F(000)	1012	
Crystal size	0.50 x 0.44 x 0.32 mm ³	
θ range for data collection	5.32 to 67.53°	
Index ranges	-19 ≤ h ≤ 17, 0 ≤ k ≤ 11, 0 ≤ l ≤ 15	
Reflections collected	16178	
Independent reflections	3383 [R(int) = 0.0305]	
Completeness to θ = 67.53°	95.6 %	
Absorption correction	Numerical	
Max. and min. transmission	0.1371 and 0.0791	
Refinement method	Full-matrix least-squares on F ²	
Data / restraints / parameters	3383 / 0 / 332	
Goodness-of-fit on F ²	1.115	
Final R indices [I > 2σ(I)]	R ₁ = 0.0211, wR ₂ = 0.0516	
R indices (all data)	R ₁ = 0.0212, wR ₂ = 0.0517	
Extinction coefficient	0.00074(5)	
Largest diff. peak and hole	0.639 and -0.452 e.Å ⁻³	

Table S2. Crystal data and structure refinement for **2**.

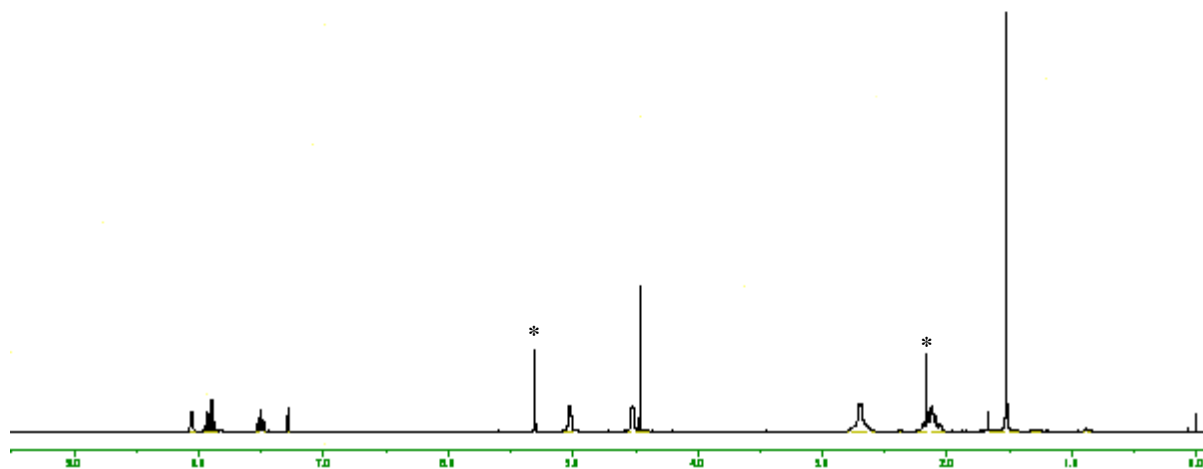
Empirical formula	C ₂₀ H ₂₄ C ₁₂ N ₄ O _{2.14} Ru	
Formula weight	526.68	
Temperature	100(2) K	
Wavelength	1.54178 Å	
Crystal system	Monoclinic	
Space group	P2 ₁ /c	
Unit cell dimensions	a = 10.72140(10) Å	α = 90°
	b = 14.1607(2) Å	β = 97.3240(10)°
	c = 14.6702(2) Å	γ = 90°
Volume	2209.09(5) Å ³	
Z	4	
Density (calculated)	1.584 Mg/m ³	
Absorption coefficient	8.173 mm ⁻¹	
F(000)	1069	
Crystal size	0.29 x 0.15 x 0.10 mm ³	
θ range for data collection	4.16 to 68.00°	
Index ranges	-12 ≤ h ≤ 12, 0 ≤ k ≤ 16, 0 ≤ l ≤ 17	
Reflections collected	18294	
Independent reflections	3921 [R(int) = 0.0163]	
Completeness to θ = 68.00°	97.6 %	
Absorption correction	Numerical	
Max. and min. transmission	0.4954 and 0.2003	
Refinement method	Full-matrix least-squares on F ²	
Data / restraints / parameters	3921 / 0 / 272	
Goodness-of-fit on F ²	0.981	
Final R indices [I > 2σ(I)]	R ₁ = 0.0194, wR ₂ = 0.0513	
R indices (all data)	R ₁ = 0.0197, wR ₂ = 0.0515	
Extinction coefficient	0.00020(3)	
Largest diff. peak and hole	0.405 and -0.295 e.Å ⁻³	

Table S3. Crystal data and structure refinement for **3**.

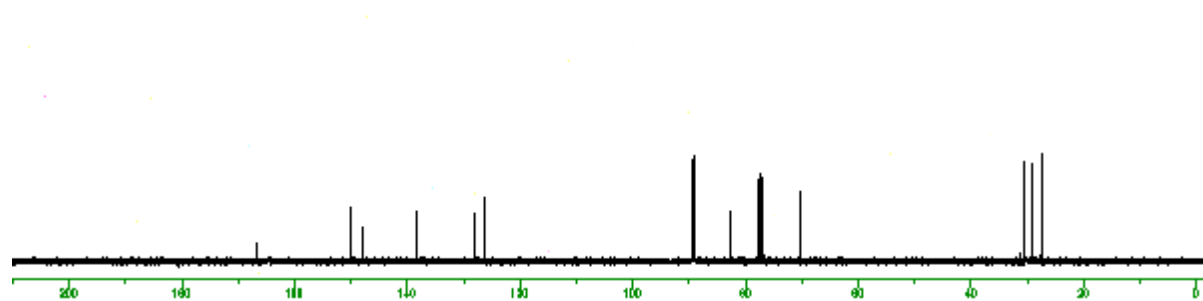
Empirical formula	C ₂₁ H ₂₆ BCl ₄ F ₄ N ₄ O ₂ Ru	
Formula weight	696.14	
Temperature	100(2) K	
Wavelength	1.54178 Å	
Crystal system	Monoclinic	
Space group	P2 ₁ /c	
Unit cell dimensions	a = 8.35260(10) Å	α = 90°
	b = 28.1943(4) Å	β = 108.2210(10)°
	c = 12.6986(2) Å	γ = 90°
Volume	2840.52(7) Å ³	
Z	4	
Density (calculated)	1.628 Mg/m ³	
Absorption coefficient	8.407 mm ⁻¹	
F(000)	1396	
Crystal size	0.55 x 0.41 x 0.05 mm ³	
θ range for data collection	3.99 to 67.75°	
Index ranges	-9 ≤ h ≤ 9, 0 ≤ k ≤ 33, 0 ≤ l ≤ 15	
Reflections collected	23226	
Independent reflections	5024 [R(int) = 0.0211]	
Completeness to θ = 67.75°	97.6 %	
Absorption correction	Numerical	
Max. and min. transmission	0.6786 and 0.0905	
Refinement method	Full-matrix least-squares on F ²	
Data / restraints / parameters	5024 / 9 / 370	
Goodness-of-fit on F ²	0.969	
Final R indices [I > 2σ(I)]	R ₁ = 0.0478, wR ₂ = 0.1237	
R indices (all data)	R ₁ = 0.0489, wR ₂ = 0.1245	
Largest diff. peak and hole	1.507 and -1.065 e.Å ⁻³	

^1H and ^{13}C NMR Spectra of Complex **1**

^1H NMR (CDCl_3 , 400 MHz)

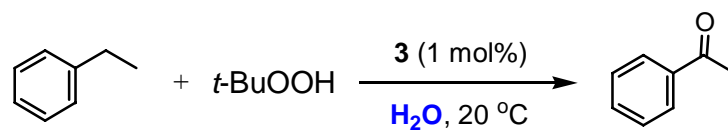


$^{13}\text{C}\{^1\text{H}\}$ NMR (CDCl_3 , 100.6 MHz)

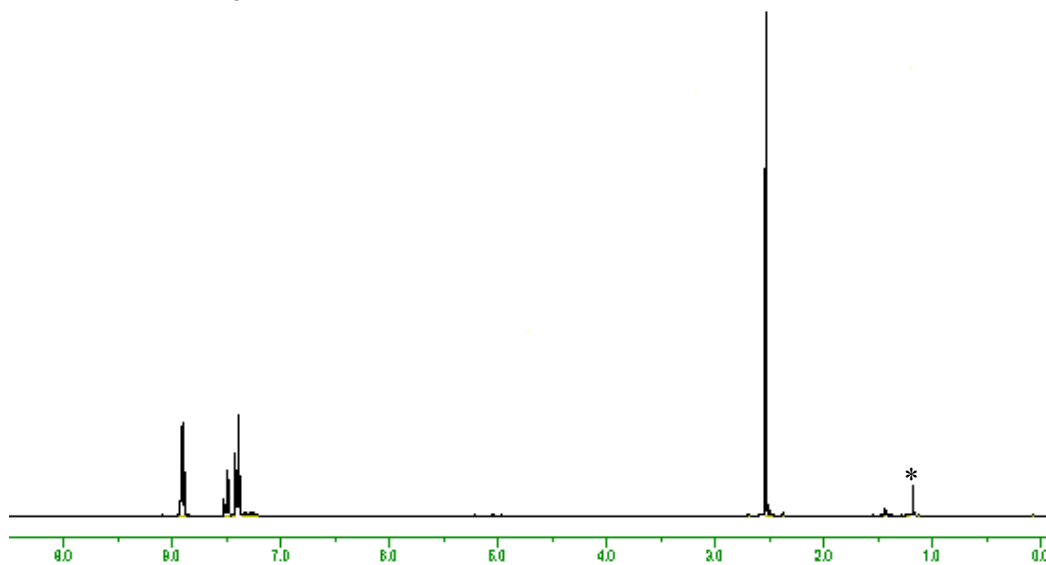


* denotes solvents.

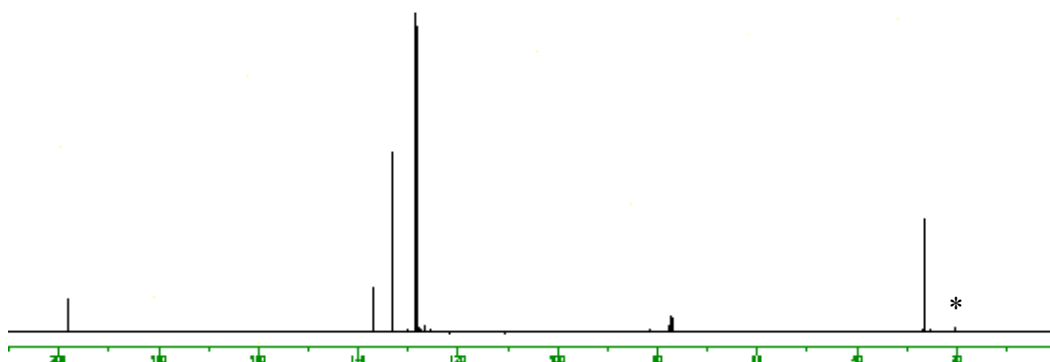
^1H and ^{13}C NMR Spectra of Selected Crude Organic Products



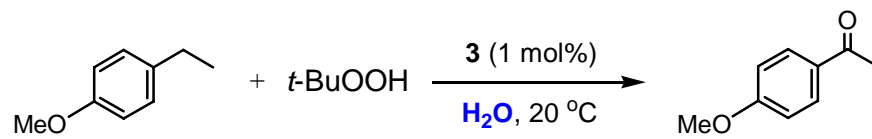
^1H NMR (CDCl_3 , 400 MHz)



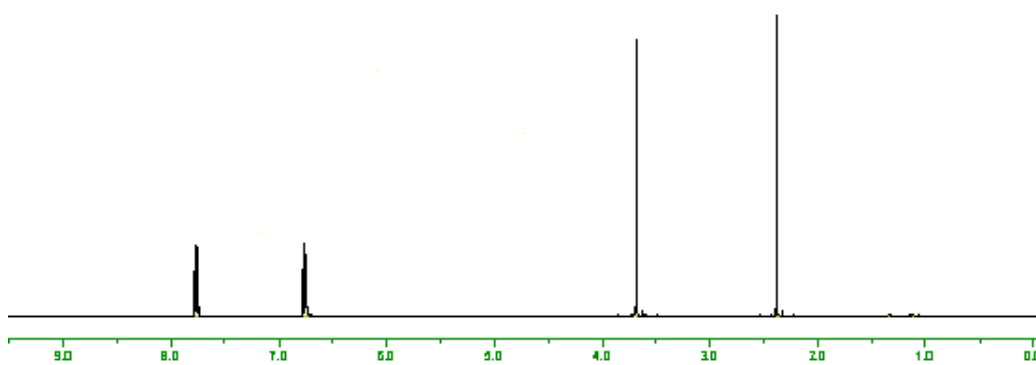
$^{13}\text{C}\{^1\text{H}\}$ NMR (CDCl_3 , 100.6 MHz)



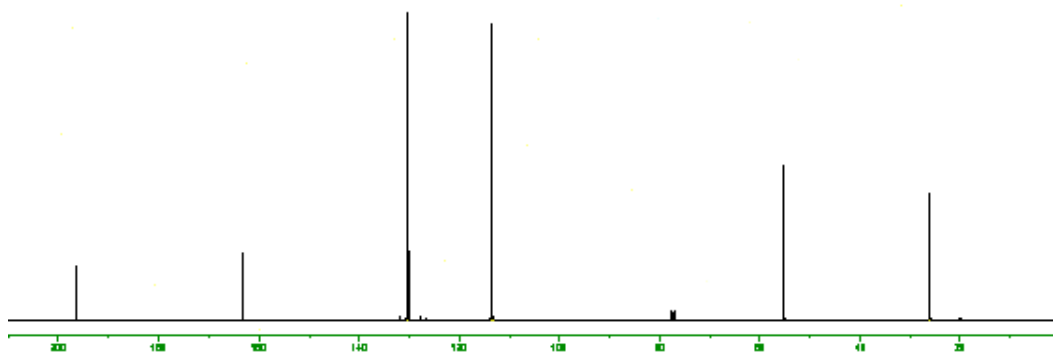
* denotes $t\text{-BuOH}$.

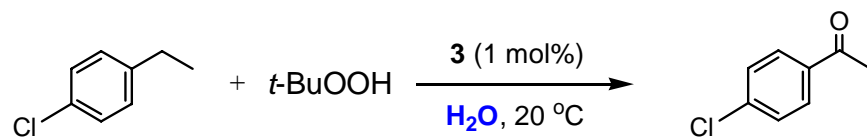


^1H NMR (CDCl_3 , 400 MHz)

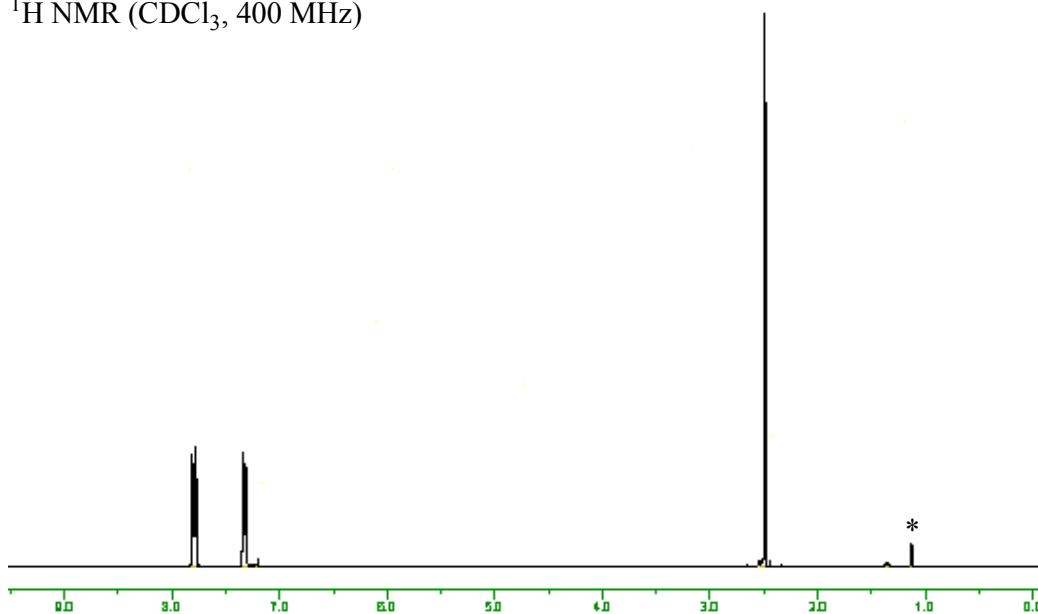


$^{13}\text{C}\{^1\text{H}\}$ NMR (CDCl_3 , 100.6 MHz)

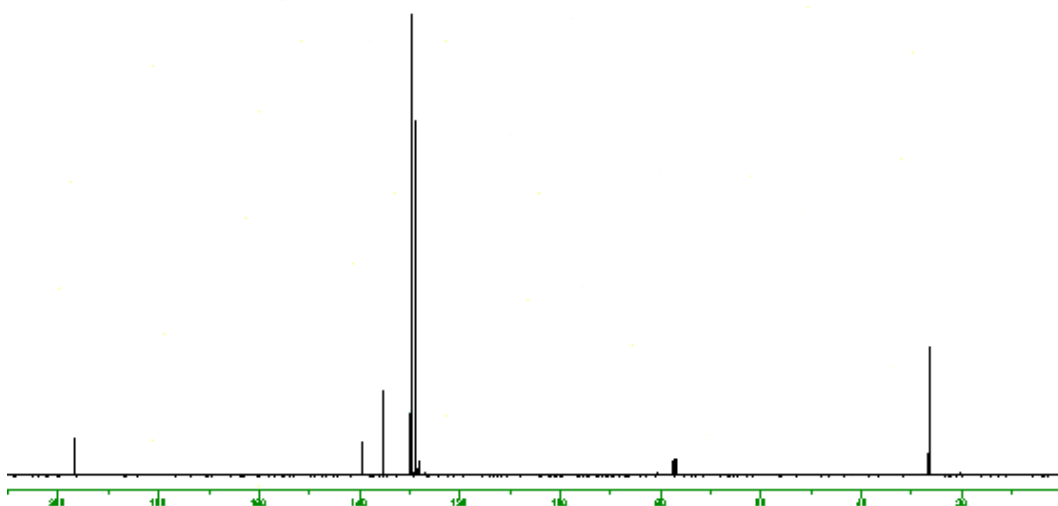




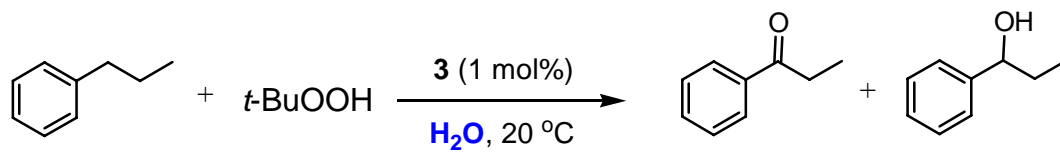
^1H NMR (CDCl_3 , 400 MHz)



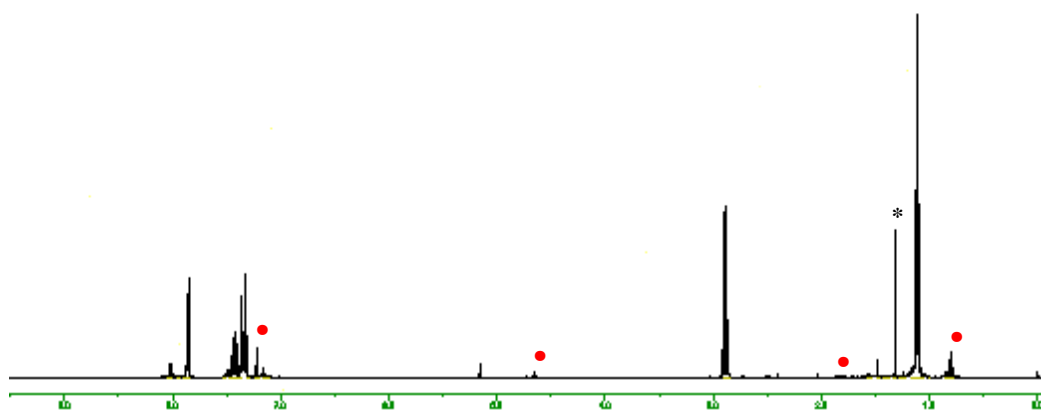
$^{13}\text{C}\{^1\text{H}\}$ NMR (CDCl_3 , 100.6 MHz)



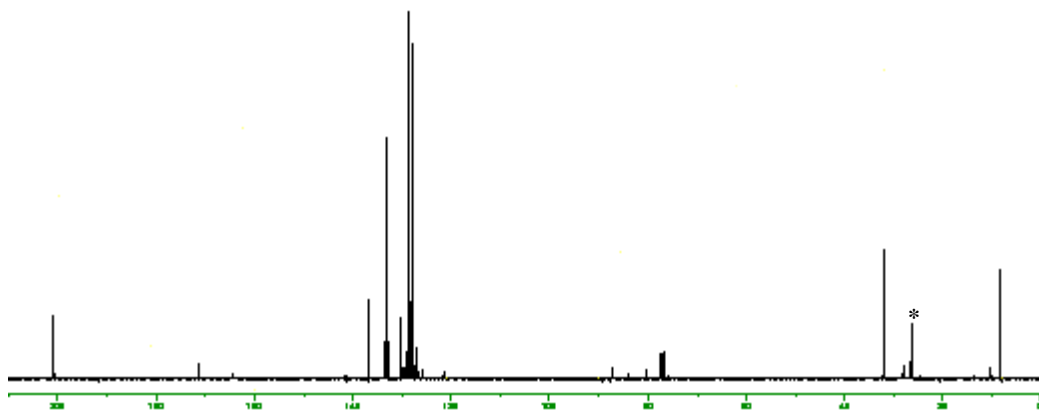
* denotes *t*-BuOH.



^1H NMR (CDCl_3 , 400 MHz)

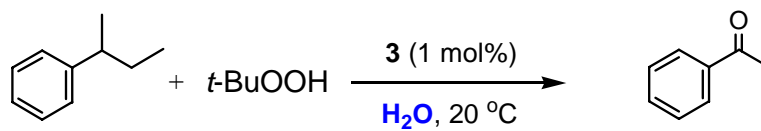


$^{13}\text{C}\{^1\text{H}\}$ NMR (CDCl_3 , 100.6 MHz)

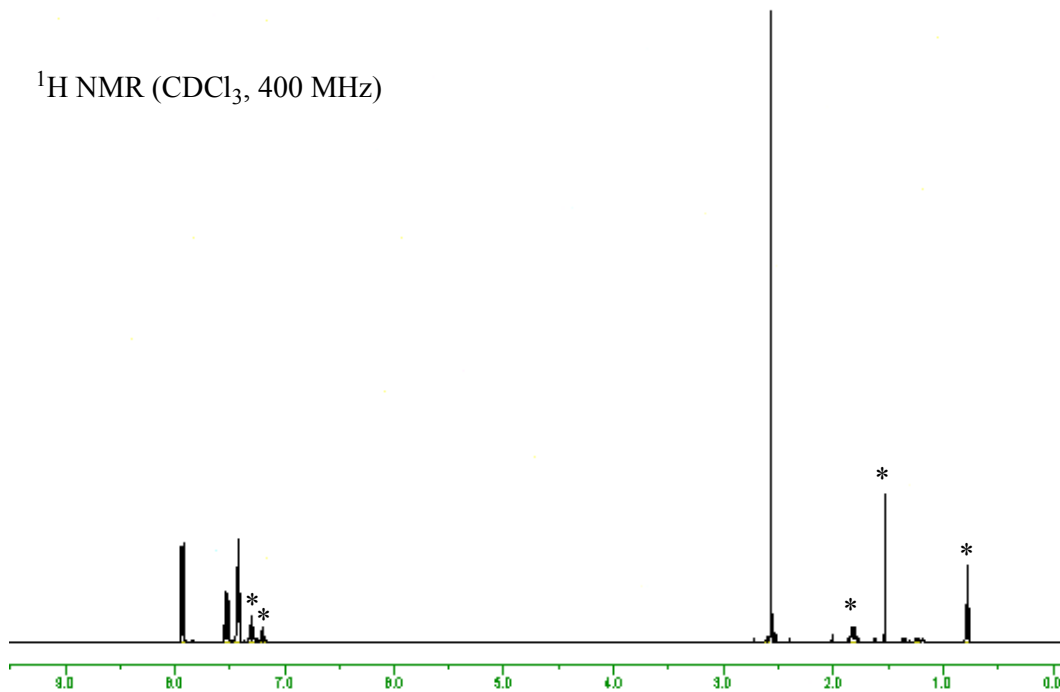


• denotes alcohol product.

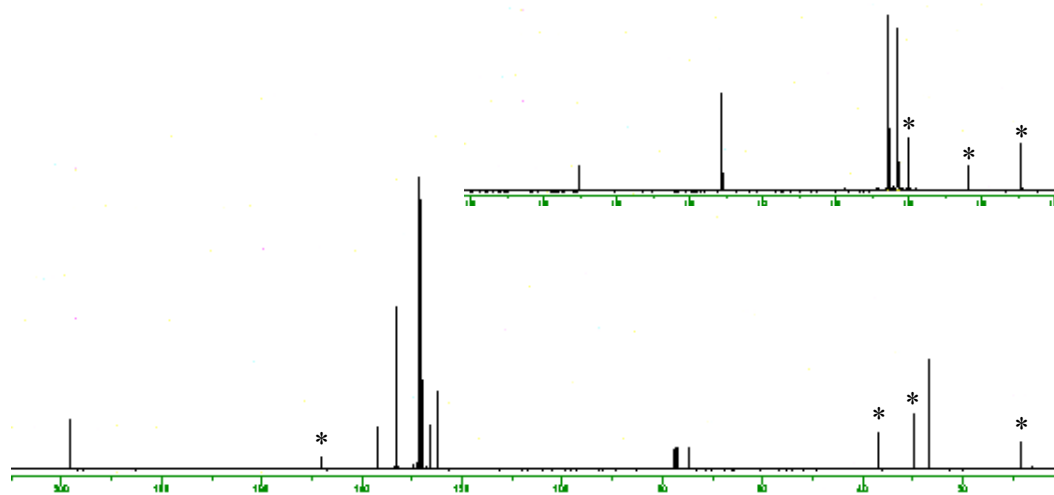
* denotes $t\text{-BuOH}$.



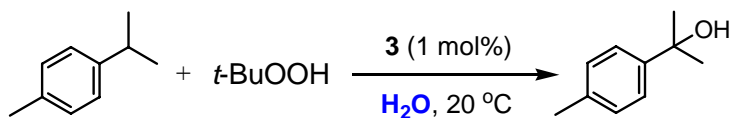
^1H NMR (CDCl_3 , 400 MHz)



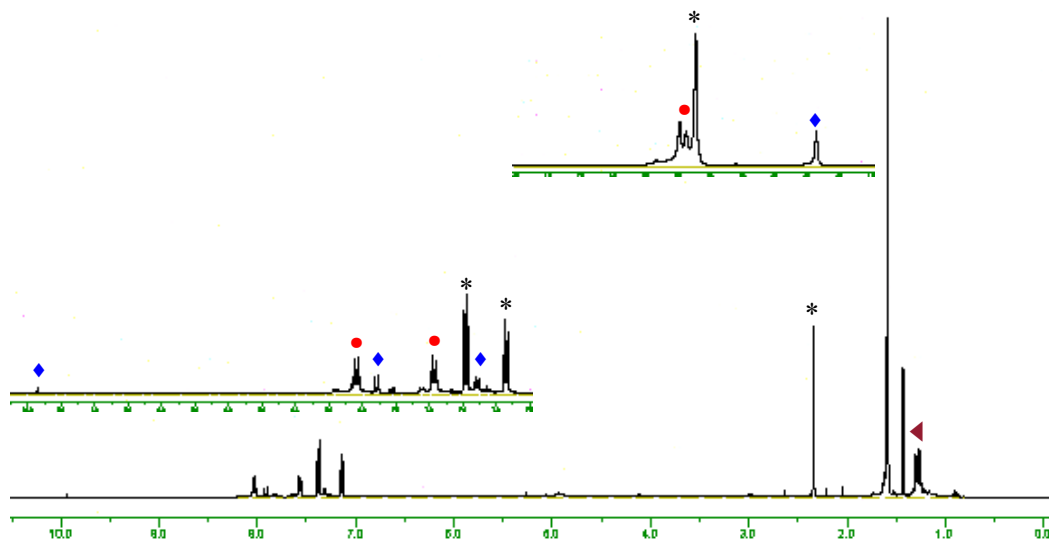
$^{13}\text{C}\{^1\text{H}\}$ NMR (CDCl_3 , 100.6 MHz)



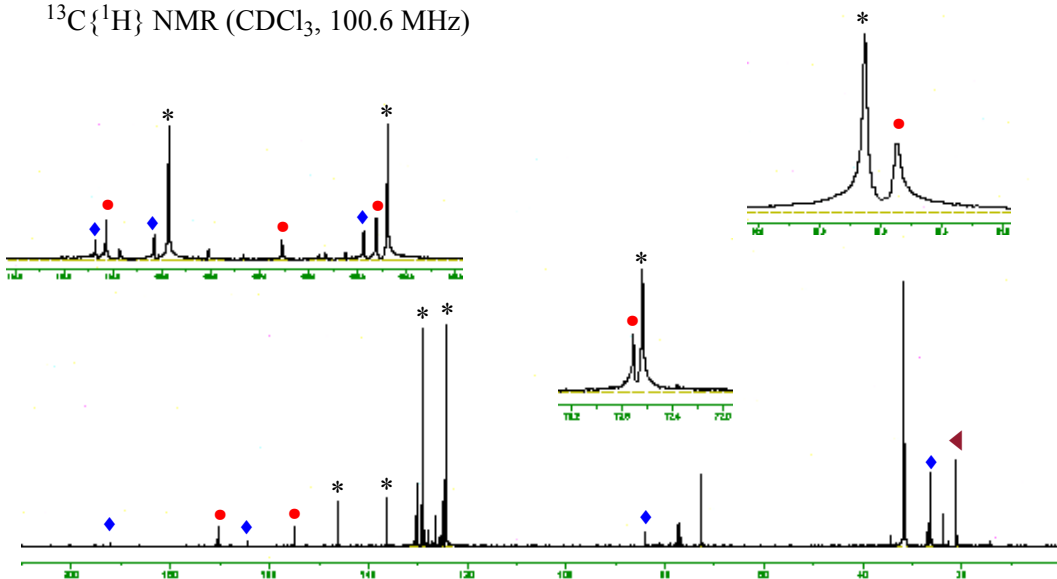
* denotes *sec*-Butylbenzene



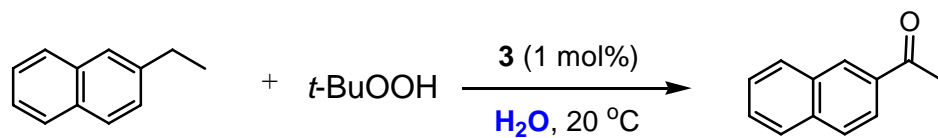
^1H NMR (CDCl_3 , 400 MHz)



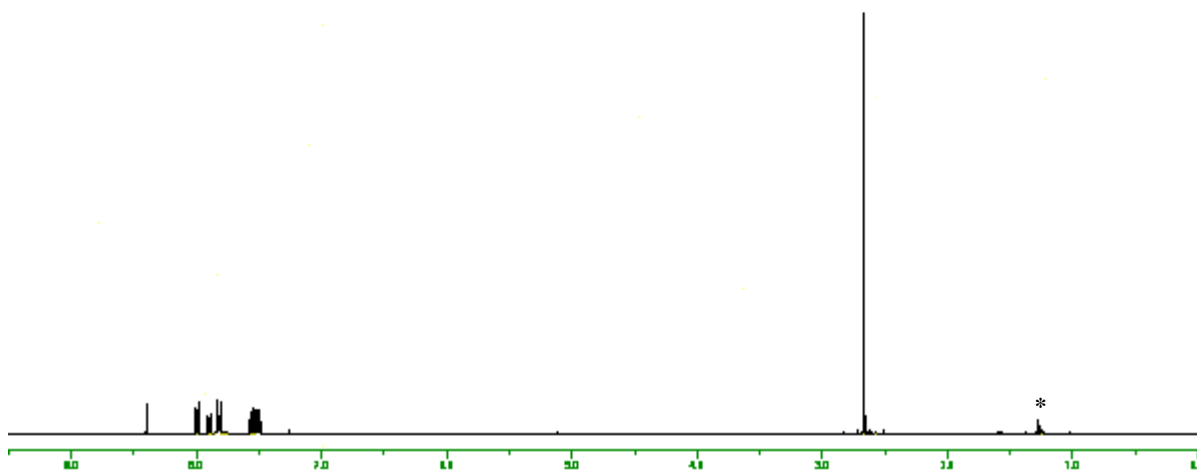
$^{13}\text{C}\{^1\text{H}\}$ NMR (CDCl_3 , 100.6 MHz)



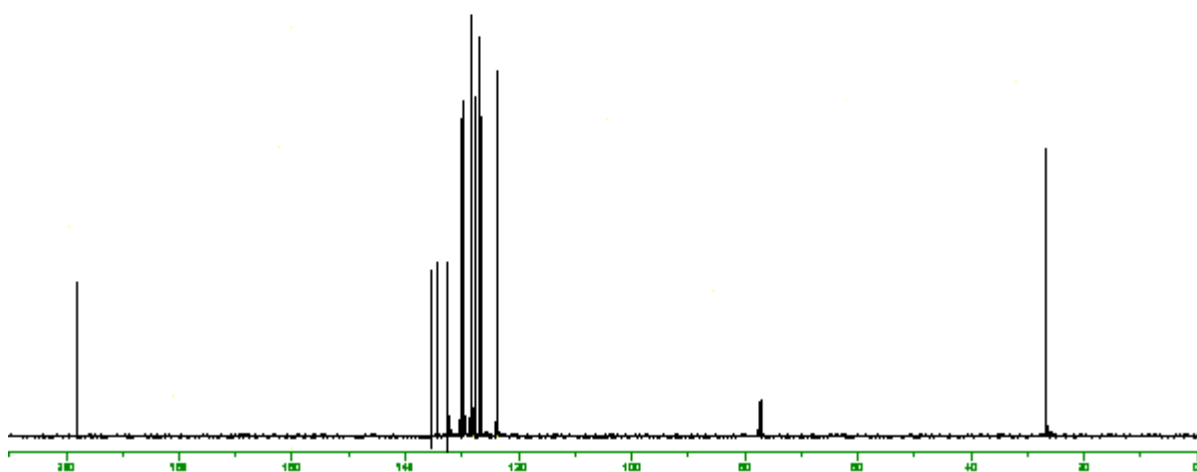
- * denotes *p*, α , α -trimethylbenzyl alcohol
- ◆ denotes 4-(1-hydroxy-1-methylethyl)benzaldehyde
- denotes 4-(1-hydroxy-1-methylethyl)benzoic acid
- ◄ denotes *t*-BuOH



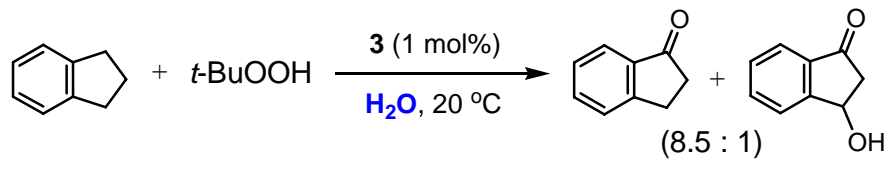
^1H NMR (CDCl_3 , 400 MHz)



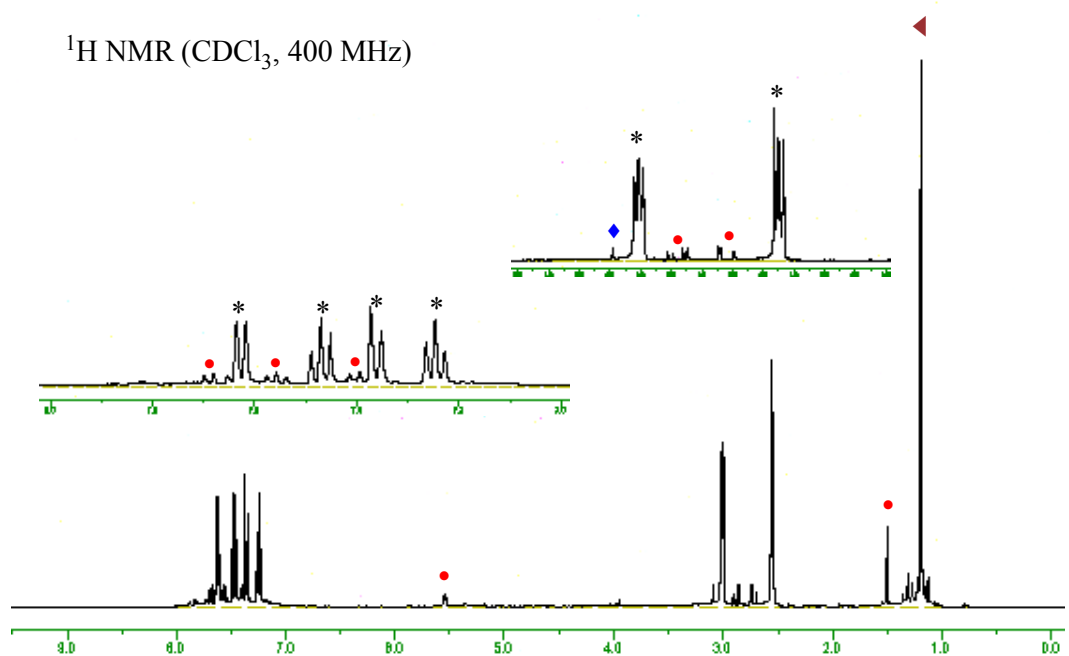
$^{13}\text{C}\{^1\text{H}\}$ NMR (CDCl_3 , 100.6 MHz)



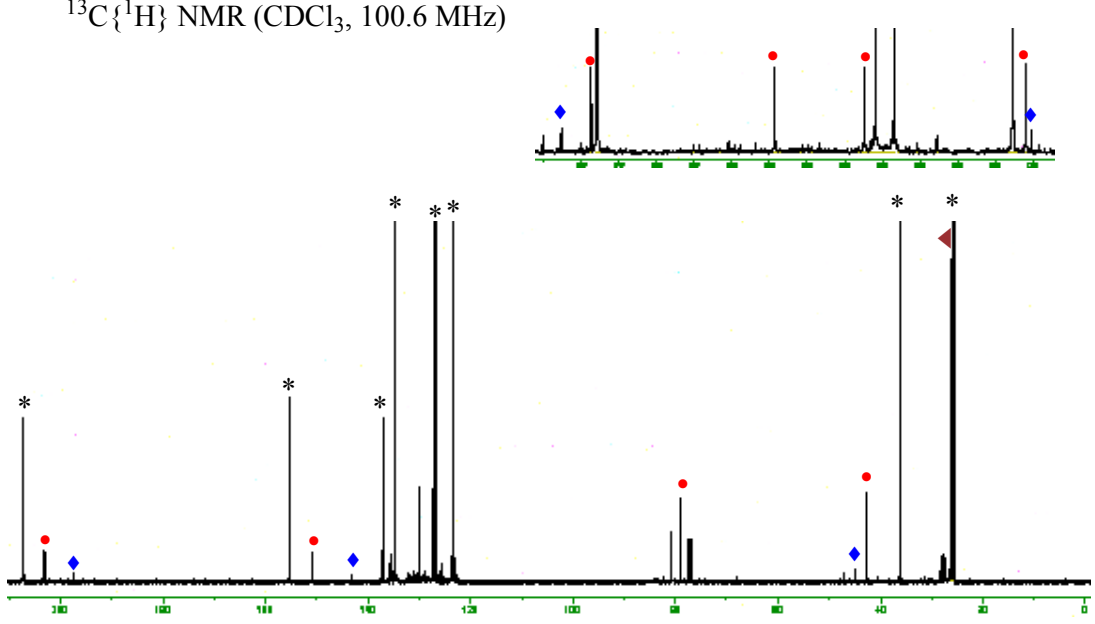
* denotes *t*-BuOH.



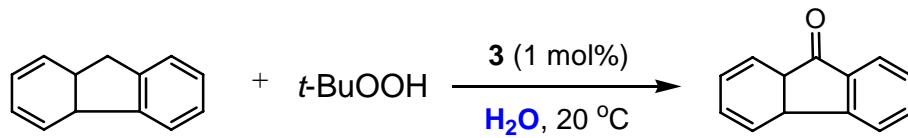
^1H NMR (CDCl_3 , 400 MHz)



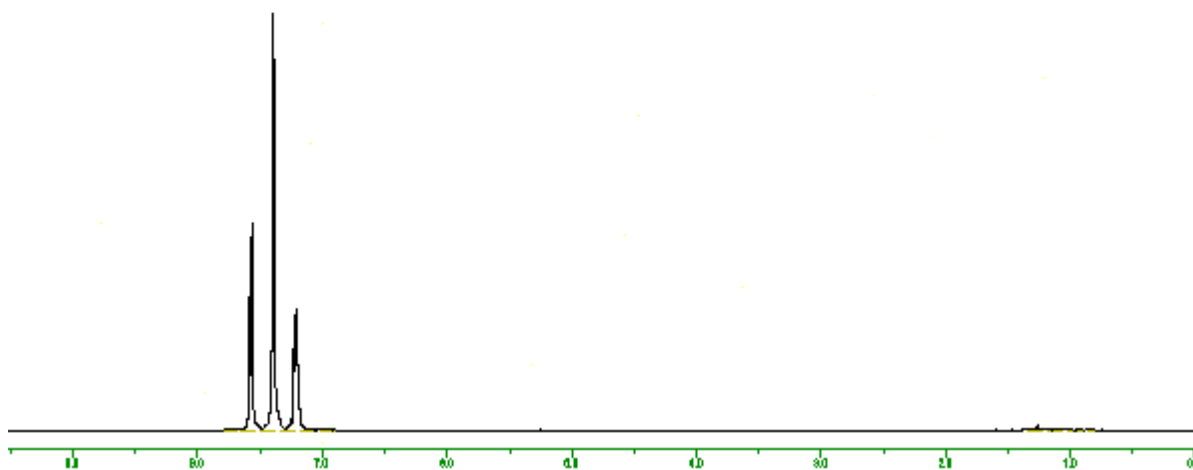
$^{13}\text{C}\{^1\text{H}\}$ NMR (CDCl_3 , 100.6 MHz)



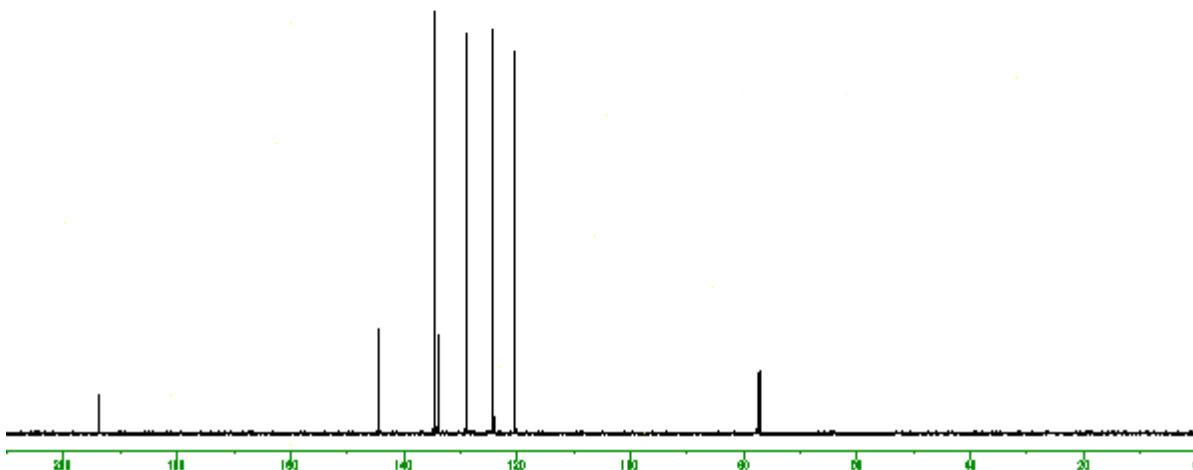
- * denotes 1-indanone
- denotes 3-hydroxy-1-indanone
- ♦ denotes 1,3-indandione
- ◄ denotes *t*-BuOH

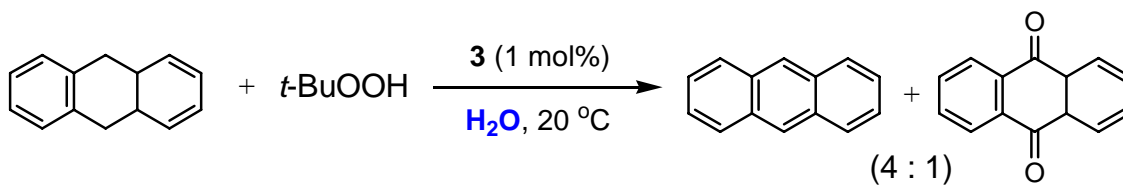


^1H NMR (CDCl_3 , 400 MHz)

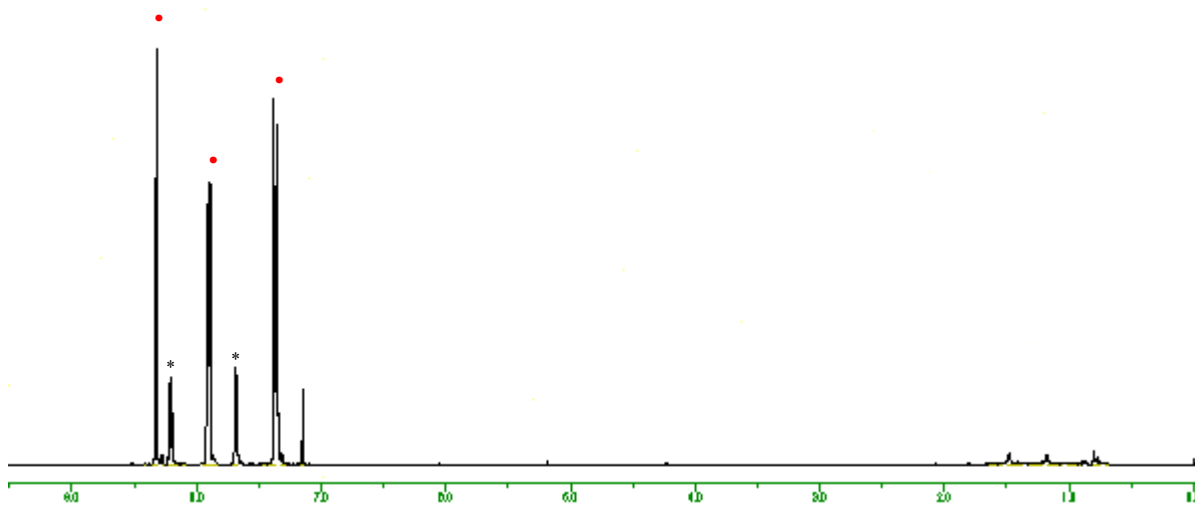


$^{13}\text{C}\{^1\text{H}\}$ NMR (CDCl_3 , 100.6 MHz)

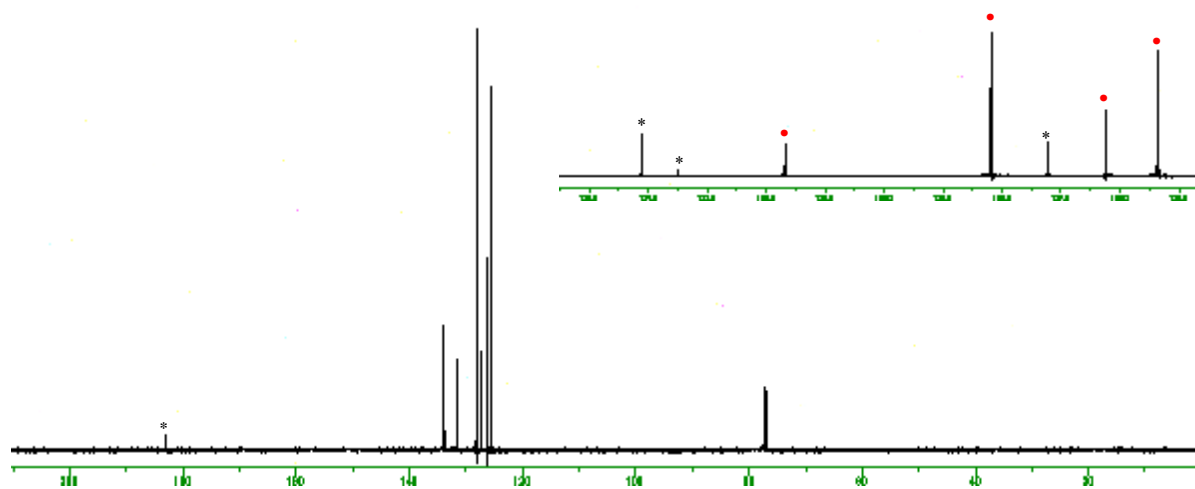




^1H NMR (CDCl_3 , 400 MHz)

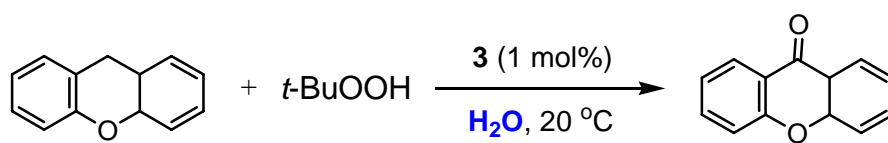


$^{13}\text{C}\{^1\text{H}\}$ NMR (CDCl_3 , 100.6 MHz)

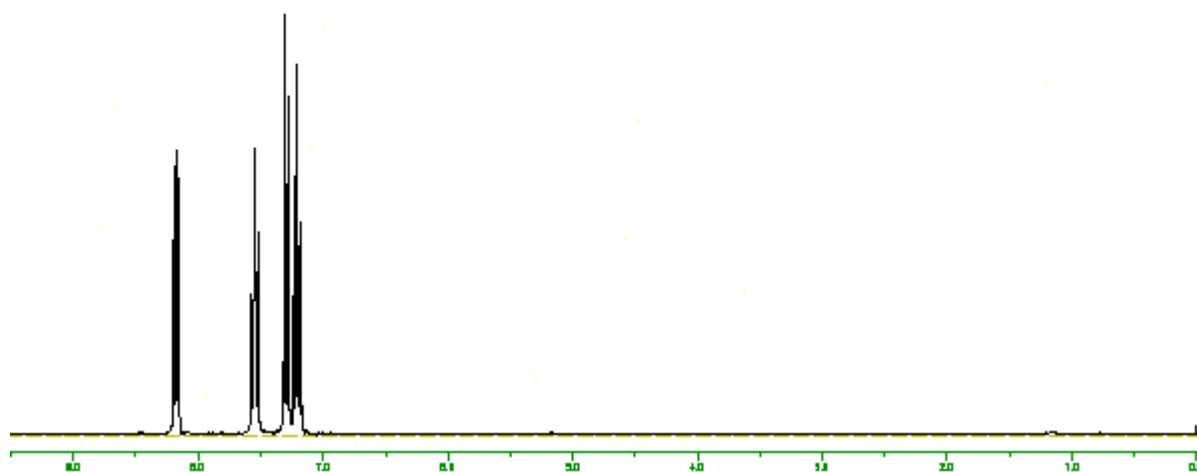


• denotes anthracene

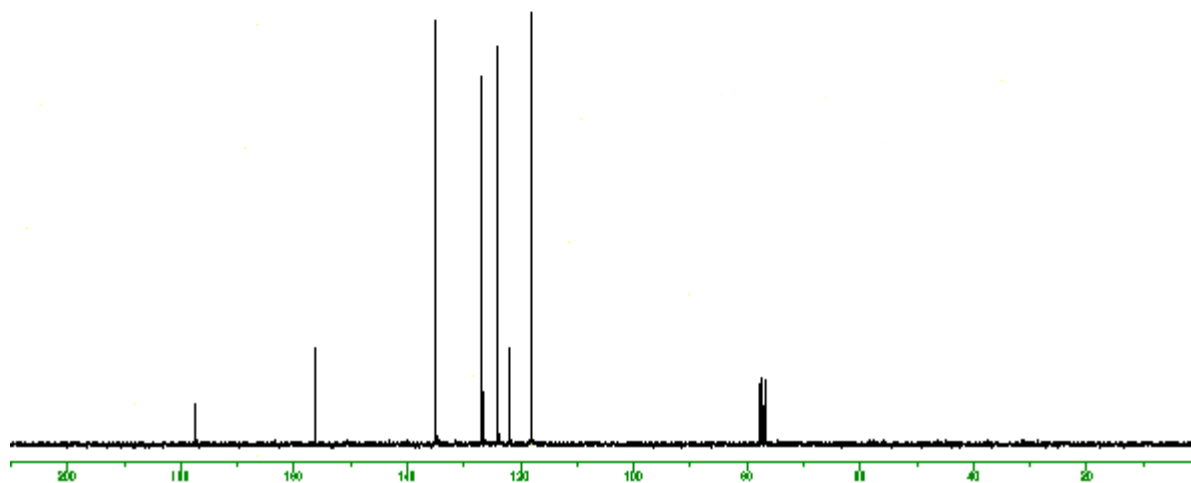
* denotes 1,4-dihydroanthraquinone

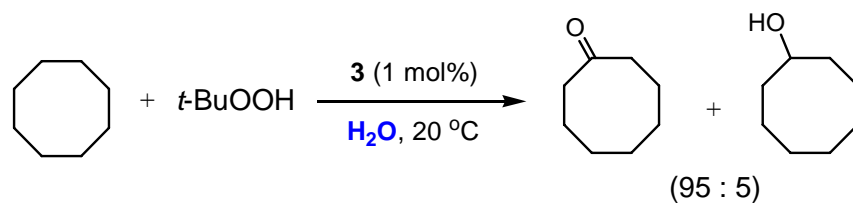


^1H NMR (CDCl_3 , 400 MHz)

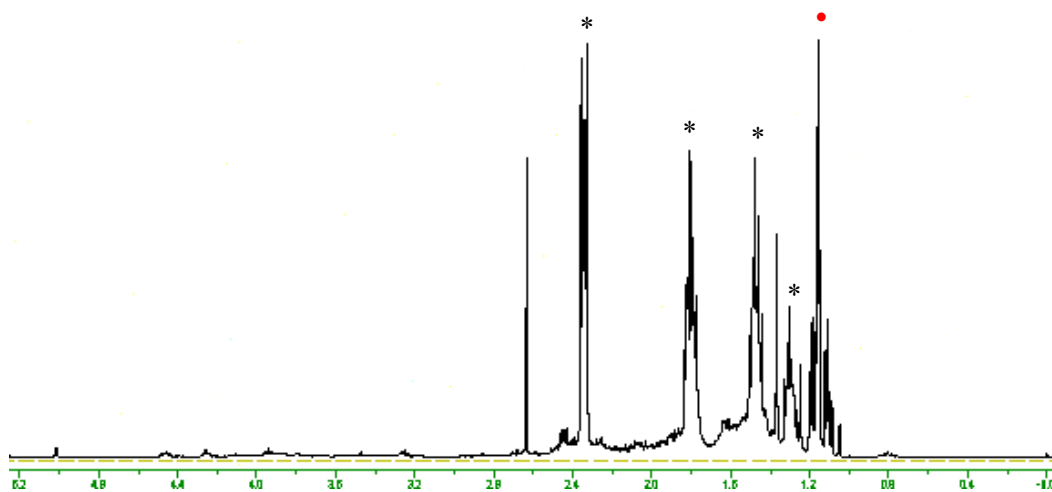


$^{13}\text{C}\{^1\text{H}\}$ NMR (CDCl_3 , 100.6 MHz)

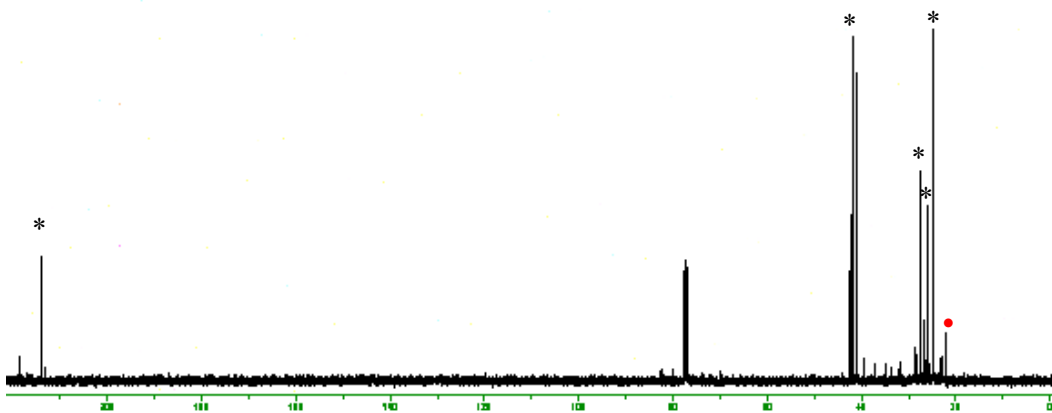




$^1\text{H NMR}$ (CDCl_3 , 400 MHz)



$^{13}\text{C}\{^1\text{H}\}$ NMR (CDCl_3 , 100.6 MHz)



* denotes cyclooctanone
 • denotes $t\text{-BuOH}$
 contains cyclooctanol and diketons